Aus dem Fachbereich Medizin
der Johann Wolfgang Goethe-Universität
Frankfurt am Main

betreut am
Zentrum der Neurologie und Neurochirurgie
Klinik der Neurologie
Funktionsbereich Neuroonkologie
Prof. Dr. Joachim P. Steinbach

Hemmung der oxidativen Phosphorylierung führt zu Bevacizumabresistenz in Glioblastomzellen

Dissertation
zur Erlangung des Doktorgrades der Medizin
des Fachbereichs Medizin
der Johann Wolfgang Goethe-Universität
Frankfurt am Main

vorgelegt von
Jule Anna Eriksson

aus Mainz

Frankfurt am Main, 2019

Dekan: Prof. Dr. Josef Pfeilschifter

Referent: Prof. Dr. Joachim Steinbach

Korreferent: Herr Prof. Dr. Donat Kögel

2. Korreferent: Herr Prof. Dr. Bernhard Brüne

Tag der mündlichen Prüfung: 05.12.2019

Inhaltsverzeichnis

Zusammenfassung

Der VEGF-neutralisierende Antikörper Bevacizumab ist ein wichtiger Bestandteil der modernen Tumortherapie [1]. Auch in der Glioblastom Therapie wird Bevacizumab eingesetzt, da in klinischen Studien eine Verlängerung des progressionsfreien Überlebens beobachtet wurde. Leider entwickeln sich schnell Resistenzen und das Gesamtüberleben konnte durch Bevacizumab in der Erstlinientherapie von Glioblastomen nicht verlängert werden [2].

Die genaue Wirkungsweise von Bevacizumab und somit auch die Resistenzentwicklung sind nur teilweise bekannt. Es wird vermutet, dass es durch Gefäßveränderungen [3] zu einer Mangelsituation und zu Hypoxie kommt [4, 5]. Einige Studien deuten darauf hin, dass es neben der Wiedererlangung einer VEGF-unabhängigen Gefäßversorgung auch zu Resistenz gegen das durch Bevacizumab hervorgerufene, von Sauerstoffmangel gekennzeichnete Mikromilieu kommt. So konnte gezeigt werden, dass Bevacizumab-resistente Tumoren einen stark glykolytischen, sauerstoff-unabhängigen Zellmetabolismus aufweisen [6, 7] und vermehrt Laktat produzieren [3]. Darüber hinaus wurde in Folge der Bevacizumab-Behandlung eine Fehlfunktion von Mitochondrien beobachtet [8, 9]. Unklar ist noch, ob die beschriebenen metabolischen Veränderungen

ein Epiphänomen der Nährstoffmangelsituation sind oder ob sie kausal mit der Resistenzentwicklung in Zusammenhang stehen.

In der vorliegenden Arbeit sollte deshalb geprüft werden, ob die metabolische Umstellung hin zu einem glykolytischen, anaeroben Phänotyp eine hinreichende Bedingung zur Entwicklung einer Hypoxie- und Bevacizumabresistenz darstellt.

Hierzu wurden Glioblastomzellen (LNT229) derart verändert, dass sie keine oxidative Phosphorylierung durchführen konnten und rein auf die glykolytische Energiegewinnung angewiesen waren (rho^0-Zellen). Diese Veränderung führte *in-vitro* zu einer Hypoxieresistenz der Zellen. Außerdem waren rho^0-Zellen empfindlicher gegenüber Glukoseentzug und einer Behandlung mit dem Glykolyse-Inhibitor 2-Deoxyglucose (2DG). Des Weiteren waren im Mausmodell intrakranielle rho^0-Tumorxenografts resistent gegenüber Bevacizumab. Diese Resistenz konnte durch zusätzliche Therapie mit 2DG wieder aufgehoben werden.

Somit konnte in der vorliegenden Arbeit gezeigt werden, dass die Hemmung der oxidativen Phosphorylierung zu einem glykolytischen Phänotyp führt, der hinreichend ist, um eine Hypoxieresistenz und in Folge dessen eine Bevacizumabresistenz in Glioblastomzellen zu verursachen. Dies lässt einen kausalen Zusammenhang zwischen bereits in anderen Studien beschriebenen metabolischen Veränderungen und einer Bevacizumabresistenz in Tumoren vermuten. Der zelluläre Glukosestoffwechsel ist damit ein vielversprechender therapeutischer Angriffspunkt zur Vermeidung und Überwindung einer Bevacizumabresistenz.

Summary

Bevacizumab, a VEGF Antibody, is frequently used in modern tumor therapy [1]. In glioblastoma therapy it showed promising response rates with a significant improvement of progression-free survival. Unfortunately, the response is only transient and recent clinical studies did not find an improvement of overall survival after first-line bevacizumab therapy in glioblastoma [2].

How bevacizumab affects tumor cells and how they become resistant remains unclear. It has been suggested that bevacizumab causes vessel rarefaction [3] and hypoxia [4, 5].

There is growing evidence that besides VEGF independent revascularization, tumor cells develop bevacizumab resistance by adapting to the hypoxic microenvironment. Recent studies could show that bevacizumab resistant tumors exhibit a glycolytic, oxygen-independent cell metabolism [6, 7] with increased lactate production [3]. Moreover, following bevacizumab treatment a destruction of mitochondrial function was found [8, 9].

However, it remains unclear if these changes are an epiphenomenon of adaptation to metabolic deprivation or a causal mechanism to develop resistance.

The presented work therefore addressed if a metabolic switch towards a glycolytic phenotype is sufficient to cause bevacizumab resistance.

To achieve this metabolic alteration, mitochondria of LNT 229 glioblastoma cells were disrupted, leading to defective oxidative phosphorylation and consequent dependence on glycolysis for energy supply (rho^0 phenotype). This led to resistance against hypoxia in this cells *in-vitro*. Furthermore, rho^0 cells were more susceptible to glucose deprivation and to the glucose analogue 2DG, which acts as an inhibitor of glycolysis. In addition, intracranial rho^0 xenografts in mice were resistant against bevacizumab, and the combination of bevacizumab with 2DG abolished bevacizumab resistance.

In conclusion, we showed that suppression of oxidative phosphorylation led to a glycolytic phenotype and indeed was sufficient to cause resistance against hypoxia and bevacizumab in glioblastoma cells. By this, a causal relationship between previously described metabolic alterations towards a more glycolytic phenotype and bevacizumab resistance is likely. Conversely, glucose metabolism of tumor cells becomes an interesting approach to avoid or overcome bevacizumab resistance in tumors.

Abkürzungen

2DG	2-Deoxyglucose
2DG-6-P	2-Deoxyglucose-6-Phosphat
CAIX	Carbonic anhydrase 9
FLAIR	fluid attenuated inversion recovery
GLS2	Glutaminase 2
GLUT1	Glukosetransporter-1
HIF1α	Hypoxia-inducible factor 1-alpha
LDH	Laktathydrogenase
LDHA	Laktathydrogenase A
MCT1	Monocarboxylat-Transporter 1
MRT	Magnetresonanztomografie
NAD+	Nicotinamid-Adenin-Dinukleotid
PBS	Phosphate buffered saline
ROS	Reactive oxygen species
VEGF	Vaskular endothelial growth factor

Übergreifende Zusammenfassung

Glioblastome sind die häufigsten bösartigen primären Hirntumoren. Die Inzidenz beträgt 3/100 000 pro Jahr, mit einem medianen Erkrankungsalter von 64 Jahren [10].

Die Prognose von Glioblastomen ist trotz Behandlung sehr schlecht und stark abhängig von Alter und Allgemeinzustand des Patienten sowie der Therapie. Die Standardtherapie umfasst derzeit eine Resektion oder Biopsie, gefolgt von einer Radiochemotherapie und anschließender Chemotherapie mit Temozolomid; das mittlere Überleben beträgt hierunter weniger als 15 Monate [12]. Für die Rezidivtherapie ist kein fester Standard etabliert. Möglich sind eine erneute Resektion, Strahlentherapie, oder Temozolomid-Chemotherapie. Alternativ oder ergänzend können auch Lomustin sowie Bevacizumab eingesetzt werden [13].

Bevacizumab ist ein VEGF-neutralisierender Antikörper mit antiangiogener Wirkung, der inzwischen bei einigen Tumorentitäten fester Bestandteil der modernen Tumortherapie ist. In den letzten Jahren hat Bevacizumab auch in der Glioblastom Therapie zunehmend an Bedeutung gewonnen [14]. In der Rezidivsituation zeigte sich ein verlängertes progressionsfreies Überleben [29, 30]. Außerdem ist unter einer Bevacizumab-Therapie weniger Einsatz von Cortison notwendig, sodass indirekt möglicherweise die Lebensqualität verbessert wird [31]. Leider kommt es sehr rasch zur Resistenzentwicklung. Dementsprechend ergaben große klinische Studien, dass Bevacizumab in der Therapie von Glioblastomen nicht zur Verlängerung des Gesamtüberlebens führt [15, 16, 30]. Mechanismen der Resistenzentwicklung gegenüber Bevacizumab sind weiterhin unklar. Es lassen sich zwei grundlegende Resistenzmechanismen vermuten [17]. Zum einen wurde postuliert, dass Bevacizumab-resistente Tumoren die Gefäßversorgung durch VEGF-unabhängige Neovaskularisierung wiedererlangen (Abb.1). Es wurden im MRT Bevacizumab-resistente Tumoren beschrieben, die viel Kontrastmittel im FLAIR positiven Areal anreichern, was histologisch einer vergleichsweise hohen Gefäßdichte im Tumor und einer geringen Expression von hypoxischen Markern wie HIF1α entsprach [1]. Zum anderen wurde eine Resistenz gegenüber der durch Bevacizumab hervorgerufenen blutgefäßarmen und hypoxischen Mangelsituation beschrieben mit hoher Invasivität der Tumorzellen (Abb.1). Klinisch wurden dem entsprechend Tumoren mit einer geringen Kontrastmittelanreicherung innerhalb des FLAIR positiven Areales beschrieben, die histologisch eine geringe Gefäßdichte und Expression von hypoxischen Markern aufwiesen [1]. Diese Tumorzellen zeichnen sich durch eine Hypoxieresistenz und durch einen sauerstoffunabhängigen Zellstoffwechsel aus.

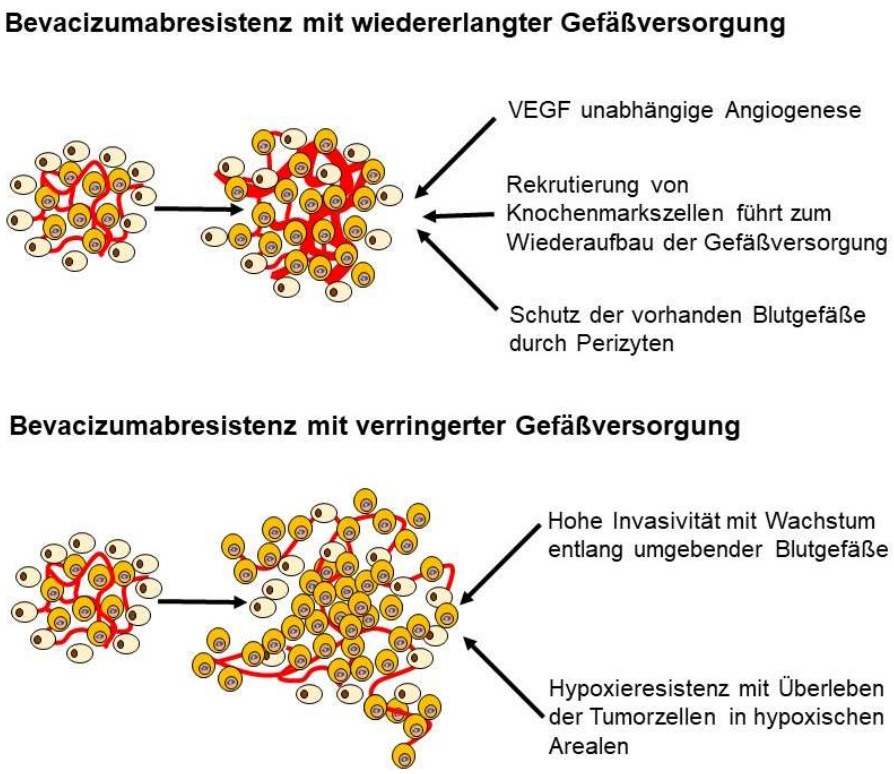

Abb.1. Mechanismen der Bevacizumabresistenz im Glioblastom

Oben: Wiedererlangung der Gefäßversorgung durch VEGF unabhängige Vorgänge. Unten: Resistenz gegenüber der Mangelsituation bei weiterhin unzureichender Gefäßversorgung.

Modifiziert nach Favaro et al. [17]

Dazu passend gibt es zunehmend Hinweise, dass Bevacizumab-resistente Glioblastome eine erhöhte glykolytische Aktivität haben und vermehrt glykolytische Enzyme exprimieren [11, 18, 7, 3]. Außerdem zeigte sich, dass die Behandlung mit Bevacizumab zum Verlust wichtiger Atmungskettenbestandteile führen kann [3, 9].

Ein veränderter Zellmetabolismus mit verstärkter Glykolyse ist ein bekanntes Phänomen während der Tumorentstehung und Malignisierung. In gesunden Körperzellen wird Glukose unter Verbrauch von Sauerstoff in der Glykolyse und anschließend über den Citrat-Zyklus und die Atmungskette abgebaut (oxidative Phosphorylierung). Bei unzureichender Sauerstoffversorgung (Hypoxie) kann die Atmungskette nicht genutzt werden und die Energiebreitstellung erfolgt rein über die Glykolyse mit abschließender

Milchsäuregärung, wobei Laktat entsteht (Abb.2). 1920 wurde erstmals durch Otto Warburg beobachtet, dass Tumorzellen einen gesteigerten Glukoseverbrauch und eine erhöhte Laktatproduktion aufweisen (Warburg-Effekt) [19]. In Tumorzellen sind häufig wichtige Enzyme der Glykolyse hochreguliert. Dabei nehmen insbesondere Glukosetransporter-1 (GLUT1) [20], Hexokinase [15], sowie die Laktatdehydrogenase (LDH) [16] eine wichtige Stellung ein. Diese Proteine wurden deshalb auch zur Charakterisierung der Zelllinie in der vorliegenden Arbeit herangezogen. Weshalb Tumorzellen, die energetisch deutlich effizientere oxidative Phosphorylierung häufig ausschalten, hat vermutlich mehrere Ursachen. Der Abbau von Pyruvat zu Laktat durch die Laktatdehydrogenase ermöglicht eine rasche Regeneration von NAD^+ und verhindert das Anreichern von Pyruvat. Die Zelle kann hierdurch rasch viel Glukose aufnehmen, um sie über die Glykolyse sowie den Pentosephosphatweg zu verstoffwechseln. Dies ist notwendig, um wichtige Intermediate für die Nucleotid-, Aminosäure- und Lipidsynthese bereitzustellen, die für Zellwachstum benötigt werden. Auch bei Hypoxie, die im Tumorgewebe häufig auftritt, könnte der Warburg-Effekt Vorteile für die Zellen bieten, da die glykolytische Energiebereitstellung sauerstoffunabhängig ist. Ferner entstehen in der Glykolyse keine Sauerstoffradikale (ROS), die bei Hypoxie vermehrt in der Atmungskette entstehen und Zelltod induzieren können.

Die metabolische Umstellung von Tumorzellen ist deshalb als Angriffspunkt für Tumortherapien von großem Interesse. Für Gliome konnte in vorherigen Studien bereits gezeigt werden, dass Restriktion von Kohlenhydraten [21] im Mausmodell die Wirkung von Bevacizumab verstärkt. Des Weiteren konnte Dichloroacetate (ein Inhibitor der Pyruvat-Dehydrogenase-Kinase), welches zur vermehrten Aktivierung der aeroben Glykolyse führt, die tumorhemmende Wirkung von Bevacizumab verstärken [22]. Aufgrund der hohen Toxizität von Dichloroacetate ist ein klinischer Einsatz in ausreichend hohen Dosen nur eingeschränkt möglich. Möglicherweise könnten andere Glykolyse-Inhibitoren wie das Pyruvatanalogon 3-Bromopyruvat oder das Glukoseanalogon 2-Deoxyglukose (2-DG) klinische Anwendung finden. Eine Studie konnte zeigen, dass Bevacizumab-resistente Tumorzellen besser auf 3-Bromopyruvat ansprechen als Bevacizumab-naive Zellen [3]. Für die Kombination von 2-DG mit Bevacizumab gibt es noch keine klinischen Untersuchungen. 2-DG ist ein Inhibitor der Hexokinase (Abb.2), der durch diese zu 2-Deoxyglukose-6-Phosphat umgebaut wird. Dieses kann nicht weiter

in der Glykolyse verstoffwechselt werden und akkumuliert somit in der Zelle [23]. Studien, die die Kombination von Strahlentherapie mit 2-DG untersuchen, zeigen eine gute Verträglichkeit des Medikamentes [24].

Die Fragestellung der hier vorliegenden Arbeit ist, ob allein die Umstellung hin zu einem glykolytischen Zellmetabolismus eine Hypoxieresistenz und damit eine Resistenz gegenüber Bevacizumab vermitteln kann. Des Weiteren sollte untersucht werden, ob eine mögliche Bevacizumab-resistenz durch Kombination mit dem Glykolyse-Inhibitor 2-Deoxygukose aufgehoben werden kann.

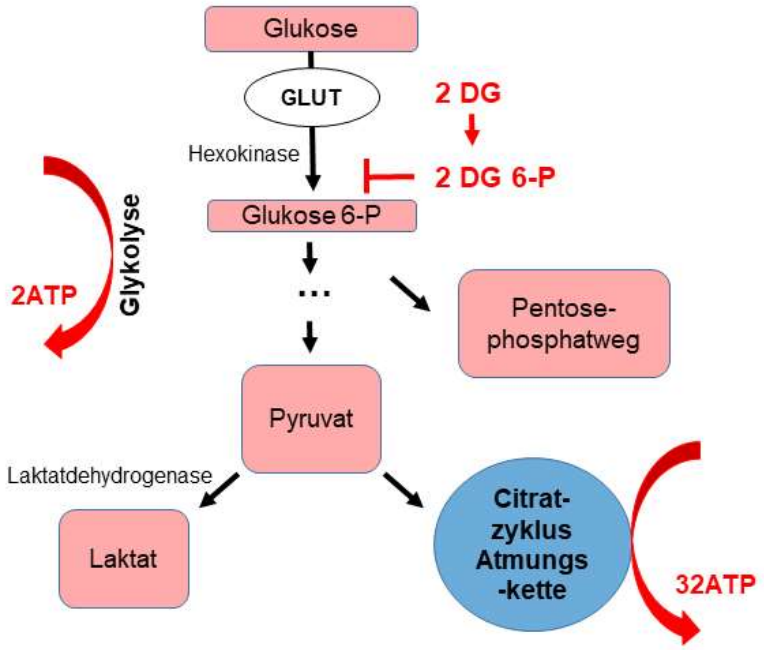

Abb. 2. Glukosestoffwechsel

Glukose wird über die Glukose-Transporter (GLUT) in die Zelle aufgenommen und durch die Hexokinase zu Glukose 6-P umgesetzt, das die Zelle nicht mehr verlassen kann. Rot ist die anaerobe Verstoffwechslung der Glukose zu Laktat oder über den Pentosephosphatweg dargestellt. Unter Anwesenheit von Sauerstoff werden diese Wege in gesunden Körperzellen gehemmt und die weitere Metabolisierung verläuft über den energieeffizienteren Citratzyklus und die sauerstoffabhängige Atmungskette (in blau dargestellt). 2-Deoxyglukose (2DG) wird durch die Hexokinase zu 2DG-6-P umgesetzt, welches das Enzym wiederum hemmt und somit die Glykolyse blockiert.

In der vorliegenden Arbeit wurden Glioblastomzellen so verändert, dass sie keine oxidative Phosphorylierung mehr durchführen konnten (rho^0 Zellen). Hierzu wurden LNT229 Zellen mit Ethidiumbromid behandelt, das zur Schädigung der Atmungskette in den Mitochondrien führte (rho^0). Wichtige Atmungskettenbestandteile wurden in den rho^0 Zellen deutlich weniger exprimiert als in den rho$^+$ Zellen. Dies ging einher mit einem herabgesetzten mitochondrialen Membranpotential und weniger ROS in den rho^0 Zellen, als Ausdruck einer gestörten Atmungskettenfunktion. Des Weiteren war die Laktat-Produktion in den rho^0 Zellen erhöht und die Zellen hatten einen höheren Glukosebedarf. Auch waren die rho^0 Zellen empfindlicher gegenüber der Behandlung mit dem Glykolyse-Inhibitor 2-DG. Am effektivsten war jedoch die Kombination von Glukoseentzug mit 2-DG. Zusammen mit der höheren Expression der Laktatdehydrogenase A (LDHA) sowie dem Glukosetransporter 1 (GLUT 1) ist dies Zeichen eines stark glykolytischen Zellmetabolismus in den rho^0 Zellen. Diese rho^0 Zellen waren resistent gegenüber Hypoxie-induzierten Zelltod. In Co-Kultur mit den rho$^+$ Zellen hatten die rho^0 Zellen unter hypoxischen Bedingungen einen deutlichen Wachstumsvorteil. Somit konnte gezeigt werden, dass in der LNT-229 Glioblastomzelllinie ein Ausschalten der oxidativen Phosphorylierung zu Verstärkung der Glykolyse und zu einer Hypoxieresistenz führt.

Um zu untersuchen, ob die Atmungsketteninsuffizienz und der daraus entstandene glykolytische Phänotyp eine Resistenz gegenüber antiangiogener Behandlung vermittelt, wurde ein Tumormodell in der Maus etabliert. Zunächst wurden rho^0-und rho$^+$-Zellen subkutan implantiert. Ohne Behandlung wiesen die Zelllinien vergleichbare Wachstumsraten auf. Des Weiteren konnte gezeigt werden, dass die Atmungskettenenzyme in den rho^0-Zellen auch nach 40 Tagen subkutanen Wachstums weiterhin reduziert waren. Schließlich wurde noch untersucht, ob der Gefäßwachstumsfaktor VEGF unterschiedlich in den rho^0 und rho$^+$ Zellen exprimiert wird, was ein unterschiedliches Ansprechen auf Bevacizumab hätte erklären können. Hier zeigten sich keine signifikanten Expressionsunterschiede zwischen den Zelllinien oder den subkutanen Tumor-Xenografts. Für weitere Untersuchungen wurden Zellen intrakraniell implantiert. Nach 10 Tagen begann eine intraperitoneale Behandlung mit Bevacizumab oder PBS. Die rho$^+$ Tumoren sprachen gut auf eine Bevacizumab-Therapie an, was sich in einer Verlängerung des medianen symptomfreien Überlebens zeigte. In

den rho^0 Zellen gab es jedoch keine Verlängerung des medianen Überlebens unter Bevacizumab-Therapie verglichen mit der PBS-Behandlung. Anschließend wurde geprüft, ob die Bevacizumabresistenz in den rho^0 Zellen durch Kombination von Bevacizumab mit dem Glykolyse-Inhibitor 2DG aufgehoben werden kann. Hierzu wurden Tiere mit rho^0-Tumoren zunächst drei Tage mit 2-DG alleine behandelt und anschließend einmal pro Woche entweder weiter mit 2-DG alleine oder der Kombination mit Bevacizumab. Als Kontrolle wurden eine alleinige Bevacizumab-Therapie oder keine Therapie (PBS-Behandlung) durchgeführt. Die alleinige Therapie mit 2-DG zeigte keine Verbesserung des Gesamtüberlebens in den Tieren mit rho^0-Tumoren. Die Kombination von 2-DG mit Bevacizumab zeigte jedoch ein gutes Ansprechen. Somit wurde gezeigt, dass in Bevacizumab-resistenten rho^0-Tumoren durch Behandlung mit 2-DG wieder eine Sensitivität gegenüber Bevacizumab erlangt werden konnte.

Die Ergebnisse der vorliegenden Arbeit weisen darauf hin, dass es einen kausalen Zusammenhang zwischen einem glykolytischen Zellmetabolismus und einer Bevacizumabresistenz gibt. Wir konnten zeigen, dass allein die Unterbindung der oxidativen Phosphorylierung mit daraus folgendem glykolytischen Phänotyp ausreichend ist, um eine Bevacizumabresistenz hervorzurufen. Somit scheint ein kausaler Zusammenhang zwischen Hypoxieresistenz und Bevacizumabresistenz zu bestehen. Da Hypoxie ein wichtiges Kennzeichen in Bevacizumab behandelten Tumoren in Patienten darstellt [25, 26, 27, 22], kann postuliert werden, dass ein Wirkmechanismus von Bevacizumab die Induktion von Hypoxie ist. Während der Resistenzentwicklung gegenüber Bevacizumab könnte eine Selektion von hypoxieresistenten Zellen eine wichtige Rolle spielen. So konnte in Gliom-Zelllinien nach Behandlung durch Bevacizumab eine zunehmende Expression von HIF-1α, CAIX und GLUT1 sowie MCT1 festgestellt werden, als Ausdruck einer vermehrten Glykolyse und Hypoxieresistenz [28].

Zusammengefasst beleuchtet die vorliegende Arbeit den Stellenwert von metabolischen Veränderungen im Rahmen der Resistenzentwicklung gegenüber antiangiogenen Therapien. Sie lässt vermuten, dass eine vermehrte Glykolyse und damit verbundene Hypoxieresistenz im kausalen Zusammenhang mit der Resistenzentwicklung gegenüber Bevacizumab steht. Sie unterstützt damit den Ansatz, Bevacizumab mit Inhibitoren der Glykolyse oder mit Glukose-Restriktion zu kombinieren.

Die zur Veröffentlichung angenommene Publikation

Eriksson JA, Wanka C, Burger MC, Urban H, Hartel I, von Renesse J, Harter PN, Mittelbronn M, Steinbach JP, Rieger J. Suppression of oxidative phosphorylation confers resistance against bevacizumab in experimental glioma. J Neurochem. 144(4):421-430; 2018.

Journal of Neurochemistry

JOURNAL OF NEUROCHEMISTRY | 2018 | 144 | 421–430 doi: 10.1111/jnc.14264

ORIGINAL ARTICLE

Suppression of oxidative phosphorylation confers resistance against bevacizumab in experimental glioma

Jule A. Eriksson,*,† Christina Wanka,* Michael C. Burger,* Hans Urban,* Ines Hartel,* Janusz von Renesse,‡ Patrick N. Harter,‡ Michel Mittelbronn,‡,§ Joachim P. Steinbach* and Johannes Rieger*,¶

*Dr Senckenberg Institute of Neurooncology, Goethe University, Frankfurt, Germany

†Department of Neurology, University Hospital Basel, Switzerland

‡Edinger Institute, Goethe University, Frankfurt, Germany

§Luxembourg Centre of Neuropathology Dudelange, Luxembourg

¶Department of Neurology, Hertie Institute for Clinical Brain Research, University Hospital Tuebingen, Germany

Abstract

Although bevacizumab initially shows high response rates in gliomas and other tumours, therapy resistance usually develops later. Because anti-angiogenic agents are supposed to induce hypoxia, we asked whether rendering glioma cells independent of oxidative phosphorylation modulates their sensitivity against hypoxia and bevacizumab. LNT-229 glioma cells without functional mitochondria (rho^0) and control (rho$^+$) cells were generated. LNT-229 rho^0-cells displayed reduced expression of oxidative phosphorylation-related genes and diminished oxygen consumption. Conversely, glycolysis was up-regulated in these cells, as shown by increased lactate production and stronger expression of glucose transporter-1 and lactate dehydrogenase-A. However, hypoxia-induced cell death *in vitro* was nearly completely abolished in the LNT-229 rho^0-cells, these cells were more sensitive towards glucose restriction and the treatment with the glycolysis inhibitor 2-deoxy-D-glucose. In an orthotopic mouse xenograft experiment, bevacizumab induced hypoxia as reflected by elevated Hypoxia-inducible factor 1-alpha staining in both, rho$^+$- and rho^0-tumours. However, it prolonged survival only in the mice bearing rho$^+$-tumours (74 days vs. 105 days, $p = 0.024$ log-rank test) and had no effect on survival in mice carrying LNT-229 rho^0-tumours (75 days vs. 70 days, $p = 0.52$ log-rank test). Interestingly, inhibition of glycolysis *in vivo* with 2-deoxy-D-glucose re-established sensitivity of rho^0-tumours against bevacizumab (98 days vs. 80 days, $p = 0.0001$). In summary, ablation of oxidative phosphorylation in glioma cells leads to a more glycolytic and hypoxia-resistant phenotype and is sufficient to induce bevacizumab-refractory tumours. These results add to increasing evidence that a switch towards glycolysis is one mechanism how tumour cells may evade anti-angiogenic treatments and suggest anti-glycolytic strategies as promising approaches to overcome bevacizumab resistance.

Keywords: bevacizumab, glioma, glycolysis, hypoxia resistance, oxidative phosphorylation.

J. Neurochem. (2018) **144**, 421–430.

Received September 4, 2017; revised manuscript received November 6, 2017; accepted November 8, 2017.

Address correspondence and reprint requests to Joachim P. Steinbach, Dr Senckenberg Institute of Neurooncology, Goethe University Frankfurt, Schleusenweg 2-1 660528 Frankfurt am Main, Germany. E-mail: joachim.steinbach@med.uni-frankfurt.de

Abbreviations used: 2DG, 2-deoxy-D-glucose; CFSE, carboxyfluorescein succinimidyl ester; CO I, Cytochrome C oxidase I; CO II, Cytochrome C oxidase II; EBRG, enhancing bevacizumab-resistant glioblastoma; FCS, fetal calf serum; GFAP, glial fibrillary acidic protein; GLS-2, glutaminase 2; GLUT1, glucose transporter-1; HE, haematoxylin eosin; HIF-1α, Hypoxia-inducible factor 1-alpha; LDH-A, lactate dehydrogenase A; MRI, magnetic resonance imaging; NBRG, non-enhancing resistant glioblastoma; ND1, nicotinamidadenindinukleotid dehydrogenase subunit 1; PAA, pyruvate free medium; PBS, phosphate buffered saline; PI, propidium iodide; qRT-PCR, quantitative real time-PCR; rho$^+$, LNT-229 control cells (rho+); rho^0, LNT-229 without functional mitochondria; ROS, reactive oxygen species; TMRM, tetramethylrhodamine; VEGF, vascular endothelial growth factor.

Targeting angiogenesis is a promising therapeutic approach against cancer. Bevacizumab, a humanized antibody against vascular endothelial growth factor (VEGF), is widely used against different tumours including malignant glioma (Jain 2014). In glioma, high response rates (Friedman *et al.* 2009), prolonged progression-free survival (Friedman *et al.* 2009; Chinot *et al.* 2014; Gilbert *et al.* 2014) and sustained magnetic resonance imaging (MRI) alterations (Bahr *et al.* 2011) indicate that bevacizumab has profound biological effects on malignant glioma. However, therapy resistance almost inevitably evolves, and bevacizumab-resistant glioma are highly refractory against conventional rescue therapies (Kreisl *et al.* 2009; Rahman *et al.* 2014).

How bevacizumab exerts its effects on tumours is incompletely understood. There is increasing evidence that anti-angiogenic treatment induces hypoxia in solid tumours as glioma (Baumgarten *et al.* 2011). This assumption is based on the results of mouse xenograft models, where accumulation of Hypoxia-inducible factor 1-alpha (HIF-1α) and carboanhydrase IX could be observed in bevacizumab-treated glioma (de Groot *et al.* 2010; Favaro *et al.* 2012; Jahangiri *et al.* 2013). Our own results further support this hypothesis, showing stroke-like lesions in MRI in bevacizumab-treated glioma and histopathological findings indicative of hypoxia and atypical necrosis (Rieger *et al.* 2010).

Therefore, two types of resistance against bevacizumab can be postulated: tumours could escape therapy by inducing VEGF-independent angiogenesis (Bergers and Hanahan 2008), or tumour cells could adapt to survive under hypoxia and starvation condition. Based on the MRI appearance, two major groups of bevacizumab-resistant glioma were recently described (DeLay *et al.* 2012). One was called non-enhancing resistant glioblastoma (NBRG) because of its low proportion of gadolinium enhancement of the fluid-attenuated inversion recovery bright volume, whereas the other group, called enhancing bevacizumab-resistant glioblastoma, exhibited a higher percentage of gadolinium enhancement. The enhancing bevacizumab-resistant glioblastoma showed higher vessel density and less hypoxia, whereas non-enhancing resistant glioblastomas were characterized by a low vascularity and a high extent of hypoxia, indicative of hypoxia resistance in these tumours.

How exactly adaptation to hypoxia occurs in tumours treated with anti-angiogenic therapies is unclear. A persistent loss of mitochondrial protein complex I in bevacizumab resistant-xenografts of a colon carcinoma cell line was reported (Xu *et al.* 2013). Furthermore, mitochondria that were isolated from human gliomas were functionally disturbed after *in vitro* bevacizumab exposure (Nanegrungsunk *et al.* 2016). Recently, in ovarian and breast cancer cells, it was shown that bevacizumab-resistant cells showed increased glycolysis (Curtarello *et al.* 2015). Accordingly, in glioma cells, Keunen *et al.* demonstrated increased expression of HIF-1α and accumulation of lactate in a mouse glioma model after treatment with bevacizumab (Keunen *et al.* 2011). The authors recently extended these findings by demonstrating that bevacizumab leads to a metabolic switch towards anaerobic glycolysis (Fack *et al.* 2015). While these results suggest that bevacizumab-resistant tumours develop a more glycolytic phenotype, it is still unclear whether these metabolic alterations are causally responsible for resistance against anti-angiogenic treatments or an epiphenomenal metabolic adaptation. To examine whether inducing a glycolytic, oxidative phosphorylation-independent phenotype is sufficient to cause bevacizumab resistance, we generated glioma cells with a defective respiratory chain (rho^0-cells). These rho^0-cells are expected to be less dependent on oxygen supply. We investigated the response of these cells against hypoxia *in vitro* and against bevacizumab and 2-deoxy-D-glucose (2DG) in a mouse xenograft model.

Material and Methods

Cell lines

The human glioblastoma cell line LNT229 (ATCC Cat# CRL-2611, RRID:CVCL_0393) was kindly provided by Monika Hegi (Labor for tumor biology and genetics, Lausanne, Switzerland). The cell line derived from the LN229 cells. The LN229 cells harbor a p53 mutation (Wischhusen *et al.* 2003) while LNT229 carry the wild-type gene (Berger *et al.* 2010). The cell line has been used in our laboratory for several studies (recently by Thiepold *et al.* 2017). The LNT229 cell line is not listed as a commonly misidentified cell line (International Cell Line Authentication Committee). The cells were last authenticated just before the first animal experiment in 04/2013 (by Multiplexion, Mannheim, Germany). Cells were cultured in standard culture medium (Dulbecco's modified Eagle's medium, PAA, Coelbe, Germany) containing 10% fetal calf serum (FCS), l-glutamine, 4500 mg/L glucose, 110 mg/L sodium pyruvate, 100 IU/mL penicillin, and 100 mg/mL streptomycin. To generate LNT229 rho^0-cells and corresponding control cells (LNT229 rho$^+$), LNT229-cells were cultured for >2 months in uridine (50 μg/mL) in the absence (LNT229 rho$^+$-cells) or presence (LNT229 rho^0-cells) of ethidium bromide (200 ng/mL) as described previously (Miller *et al.* 1996). In experiments requiring defined glucose conditions, Dulbecco's modified Eagle's glucose and pyruvate-free medium was used without FCS. A quantity of 100 μg/mL pyruvate and 50 μg/mL uridine were added, glucose levels were adjusted as required.

Cells were seeded at a density of 5.7×10^4 cells/cm^2 if not otherwise specified and cultured in a humidified atmosphere in 21% O_2 at 37°C which was defined as standard conditions. Since physiological oxygen concentrations in the tissue differ from the atmospheric oxygen concentrations we defined 5% O_2 as normoxia and 0.1% O_2 as hypoxia as previously suggested (McKeown 2014).

RNA extraction and quantitative real time-PCR (qRT-PCR)

For RNA extraction, 200.000 cells were seeded in six-well plates and kept for 24 h under standard conditions in Dulbecco's modified Eagle's medium. Respectively, tumour tissue was frozen in liquid

nitrogen and pestled. Total RNA was extracted using the TRIzol extraction kit (Ambion, Carlsbad, CA, USA) according to manufacturer's protocol. First strand cDNA was synthesized using the Vilo cDNA synthesis kit (Invitrogen, Karlsruhe, Germany). To determine changes in gene expression, q-RT-PCR was performed using the IQ5 real-time PCR detection system (Biorad, Muenchen, Germany) after adding Absolute Blue Q-PCR Mastermix (Thermo Fisher Scientific, Hamburg, Germany) and the following primer pairs to the cDNA.

Primer pairs: SDHA fw 5′- CCACCACTGCATCAAATTCATG-3′, SDHA re 5′- TGGGAACAAGAGGGCATCTG-3′, ND1 fw 5′-TATGACGCACTCTCCCCTGA-3′, ND1 re 5′- GTAGCGGAATC GGGGGTATG-3′, COI fw 5′- CCCTAGACCAAACCTACGCC-3′, COI re 5′- ATGTGGTGTATGCATCGGGG-3′, COII fw 5′- CC GTCTGAACTATCCTGCCC-3′, COII re 5′-AAGCCTAATGTGG GGACAGC-3′, GLUT1 fw 5′-GATTGGCTCCTTCTCTGTGG-3′, GLUT1 re 5′-TCAAAGGACTTGCCCAGTTT-3′, LDHA fw 5′-CAGCTTGGAGTTTGCAGTTAC-3′, LDHA re 5′-TGATGGATC TCCAACATGG-3′, VEGF fw 5′-CTACCTCCACCATGCCAA GT-3′, VEGF re 5′-ATGTTGGACTCCTCAGTGGG-3′, GLS2 fw 5′-CATGATTCATCAGAAAGTGGCAT-3`, GLS2 re 5`-GCCTTT AGTGCAGTGGTGAA-3`.

Expression of the housekeeping gene SDHA (succinate dehydrogenase complex, subunit A) was used to analyse Cycle threshold (Ct) values with the $2^{-\Delta\Delta CT}$ method as described before (Vandesompele *et al.* 2002).

Mitotracker staining

Mitotracker red and green staining was carried out as described in the user's manual (Invitrogen). Briefly, cells were seeded in a 24-well plate and kept 24 h under standard conditions. Afterwards, cells were washed with phosphate buffered saline (PBS) and stained for 15 min with 25 nM mitotracker green or red in standard medium. After the staining, the medium was removed and exchanged with standard medium. Cells were immediately observed under the fluorescence microscope (Biozero, Keyence, Osaka, Japan).

Tetramethylrhodamine (TMRM) flow cytometry

Cells were seeded in a 24-well plate and incubated for 24 h under standard conditions. Afterwards, they were washed in PBS and incubated with 25 nM TMRM in medium containing 5mM glucose for 45 min at 37°C and normoxia (5% O_2). Flow cytometry was immediately performed to evaluate the membrane potential.

Oxygen consumption

Oxygen consumption was measured using the ABL-80 FLEX Blood Gas Analyser (Radiometer, Willich, Germany) as previously described (Wanka *et al.* 2012).

Reactive oxygen species (ROS) analysis

Cells were seeded in 24-well plates and incubated for 24 h under standard conditions. Thereafter, cells were washed in PBS and incubated for 20 h in medium containing 5 mM glucose. Cells were then washed twice with PBS, incubated 20 min. at normoxia (5% O_2) at 37°C with 10 μM H_2DCFDA (Invitrogen), washed with PBS and collected for flow cytometry analysis. DCF signal was analysed by BD Canto II.

Measurement of lactate production

Cells were treated with medium containing 25 mM glucose and incubated at normoxia or hypoxia (5% or 0.1% O_2) for 3 days. Cell-free supernatant was collected and lactate concentrations were measured at baseline and after the experiment using the biochemistry analyser Hitachi 917. Lactate production was calculated by subtracting values at 72 h from baseline values, and these values were normalised to protein concentrations measured at the end of the experiment.

Crystal violet assay to assess cell density

Cell density under glucose restriction and 2-DG treatment was assessed by crystal violet staining. Cells were seeded in 96-well plates with a density of 5000/well in Dulbecco's modified Eagle's medium and kept for 24 h under standard conditions to allow the cells to attach. A crystal violet staining was performed to ensure equal cell densities. Subsequently the standard medium was substituted with medium adjusted to 5, 2 or 1 mM glucose and cells were incubated for 12 h under normoxia (5% O_2) with or without 5 mM 2DG. Thereafter, a crystal violet staining was performed to evaluate cell densities (Kueng *et al.* 1989). Results were expressed as percent of cell densities under 5 mM glucose without 2DG.

Hypoxia-induced cell death

Hypoxia induced cell death was assessed by propidium iodide (PI)-flow cytometry. Cells were seated in 24-well plates and incubated for 24 h in under standard conditions. Afterwards, cells were washed in PBS and kept in medium containing 5mM glucose for 24 h under normoxia or hypoxia (5% or 0.1% O_2). 0.1% oxygen was induced using Gas Pak pouches for anaerobic culture (Becton-Dickinson, Heidelberg, Germany). This was followed by a staining with 5 μg/mL PI and subsequent flow cytometry analysis.

Carboxyfluorescein succinimidyl ester (CFSE) staining

For co-culture of the cell lines, LNT229 rho^0-cells were stained with carboxyfluorescein succinimidyl ester (BioLegend, SanDiego, CA, USA). Cells were washed gently in PBS, stained for 10 min. in PBS containing CFSE (10 μM), and thereafter incubated for 10 min in medium containing 10% FCS. Subsequently, the cells were washed, mixed in equal amounts with unstained LNT229 rho^+-cells, and 150 000 cells/well were seeded in 24-well plates. After 24 h incubation under standard conditions a flow cytometry analysis was performed to assess baseline proportions of LNT229 rho^0 and rho^+ cells. Afterwards, the co-cultures were incubated at normoxia or hypoxia (5% or 0.1% O_2) in medium containing 5mM glucose for 24 h and again stained and unstained cells were counted by flow cytometry analysis. The proportion of cells after 24 h at 5% or 0.1% O_2 was calculated relative to baseline proportions.

Animal care and tumour transplantation

Female inbred athymic nude mice (HSD: Athymic Nude-Foxn1nu, Harlan, Indianapolis, USA) were housed in groups of 4 animals per cage in a specific pathogen–free facility with a 12-h light/12-h dark cycle and given free access to food and water. All experimental procedures were approved by the local animal ethics committee (regional board Darmstadt F145/02) and conducted according to the guidelines for ethical use of animals in the Declaration of Helsinki.

A scheme of the experimental procedure is shown in Fig. 1. At the age of 6 weeks, 100 000 LNT229 rho^0- or rho$^+$-cells were injected intracranial, 2 mm right and 1 mm anterior to bregma suture; as described before (Lee *et al.* 2012). No statistical method was used to predetermine the sample size. After implantation, animals were placed into cages by a researcher blinded for the further treatment. Ten days after implantation PBS or bevacizumab (1 mg/kg) treatment was started with intraperitoneal injections twice a week (A). Animals that received 2DG treatment were injected intraperitoneal at day 7–9 with 500 mg/kg 2DG. Thereafter, 2DG or 2DG with bevacizumab was administered twice a week (B). Animals were monitored for health and behaviour three times weekly. The study was not preregistered but the primary endpoint was defined before the start and was not changed during the experiment. The primary endpoint was defined as symptomatic animals (20% weight loss, or neurological symptoms as paresis or epileptic seizures). The researcher that observed the animals was blinded for the treatment conditions. When the endpoint was reached, the animals were scarified immediately and the tumour tissue was extracted and put in paraformaldehyde for histology. One animal in the rho^0 BEV group of the first experiment did not develop any tumour, one animal in the rho^0 PBS group of the first experiment died because of anaesthesia, one animal in the rho^0 BEV group of the second experiment was sacrificed because of systemic tumour spread; these animals were excluded from the statistics. Subcutaneous tumour xenografts were implanted to observe growth kinetics and for RNA retrieval. 4000 000 cells were injected subcutaneously to the left and right side of the animals. Volume of subcutaneously implanted LNT229 rho$^+$- and rho^0-tumours was quantified at different time points by a caliper (height*height*width/2). After 40 days, three tumours per group were extracted and immediately taken into liquid nitrogen for q-PCR analysis.

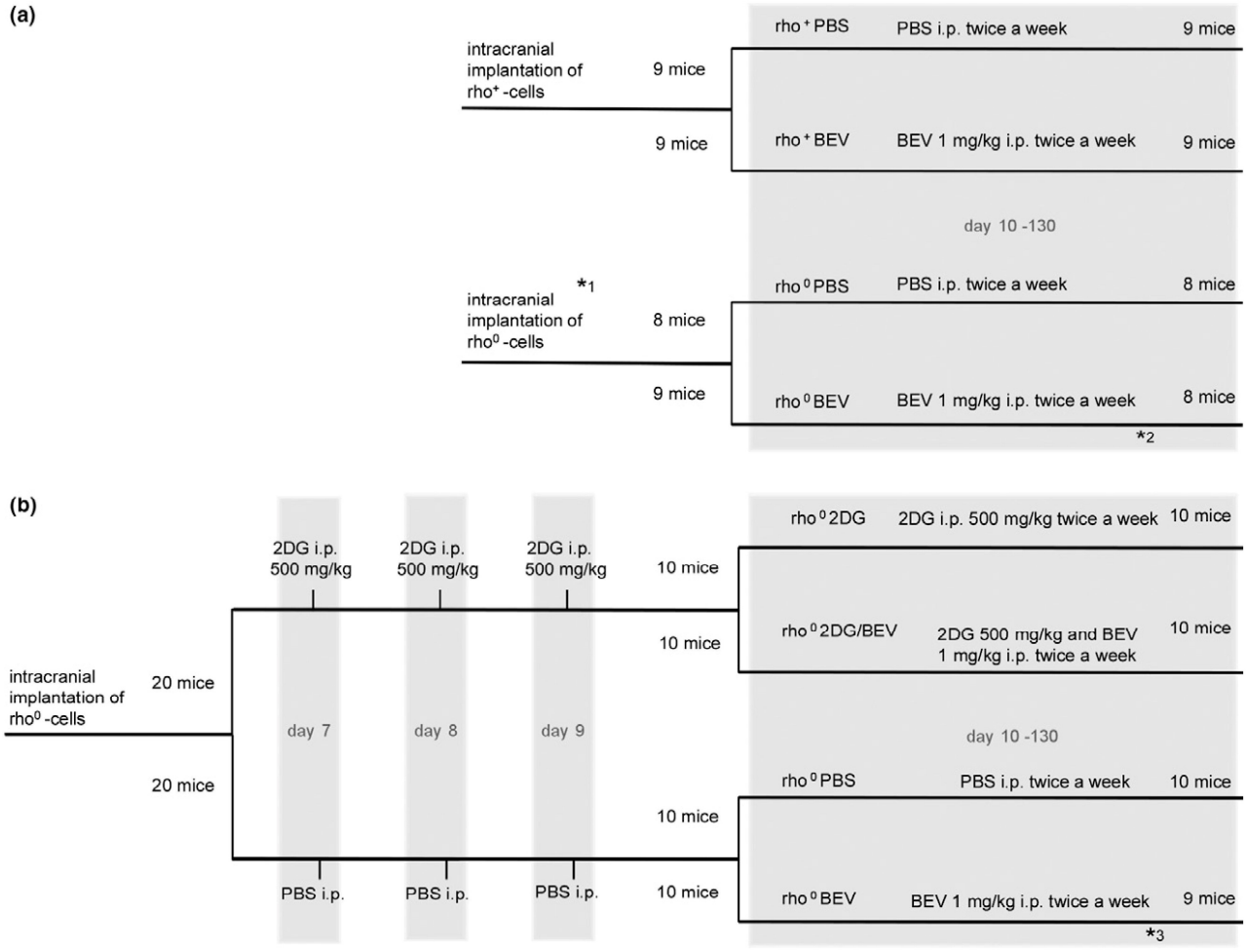

Fig. 1 Experimental procedure. (a) 100 000 LNT229 rho^0- or rho$^+$-cells were injected intracranial, 10 days after implantation phosphate buffered saline (PBS) or bevacizumab (1 mg/kg) was injected twice a week until animals were symptomatic. Two animals were excluded from the statistics, one animal from the rho^0 PBS group that died because of anaesthesia (*1), and one animal in the rho^0 BEV group that did not develop any tumour until day 130 (*2). (b) 100 000 LNT229 rho^0-cells were injected intracranial into 40 mice. 20 mice received 500 mg/kg 2DG intraperitoneal at day 7–9, the others received PBS. From day 10 until the first symptoms, 2DG injections were continued or 2DG with bevacizumab (1 mg/kg), respectively, bevacizumab alone administered twice a week. One animal in the rho^0 BEV group was excluded from the statistics because of systemic tumour spread at day 114 (*3).

Histology and immunohistochemistry

Brains were fixed in 4% paraformaldehyde in PBS and embedded in paraffin. Coronal sections (3 μm) were cut using a microtome and hematoxylin eosin stained according to standard protocols. Immunohistochemical preparations were performed using a Discovery XT automated staining module (Ventana, Tucson, AZ, USA) and standard protocols. As primary antibodies we used monoclonal rabbit anti-human lactate dehydrogenase-A (LDH-A) (dilution: 1 : 100; Cell Signalling Technology, Cambridge, UK, Cat# 3582S RRID:AB_2066887), polyclonal rabbit anti-human HIF1α (dilution: 1 : 100, Novus Biologicals, Littleton, CO, USA, Cat# NB100-134 RRID:AB_350071), and polyclonal rabbit anti-mouse glial fibrillary acidic protein (dilution: 1 : 5000, Dako, Hamburg, Germany, Cat# Z0334, RRID:AB_10013382)

Blinding

Blinding was performed for the animal experiments as described above, for all other experiments no blinding was performed.

Statistics

Shapiro–Wilk test was performed as assessment of normality for all experiments, except for survival analysis. All except oxygen consumption were normally distributed (defined as $p > 0.05$) and were analysed for significance using unpaired student's *t*-test. Mann–Whitney-U Test was used to analyse oxygen consumption. All numerical data were expressed as mean ± SEM. Survival analysis was done with Kaplan–Meier statistics and log-rank (mantel-cox) test. No test for outliners was conducted. No randomization methods were employed. Differences were considered significant at a *p*-value of < 0.05. Levels of significance were indicated as follows: $*p < 0.05$, $**p < 0.01$, $***p < 0.001$.

Results

LNT-229 rho^0-cells are characterized by reduced oxygen consumption, increased glycolysis, and sensitivity towards 2DG

To deplete mitochondrial DNA in glioblastoma cells, the glioblastoma cell line LNT-229 was cultured for 2 months in the presence of ethidium bromide and uridine (LNT-229 rho^0-cells), (Miller *et al.* 1996). The expression of mitochondrial encoded genes of the respiratory chain complex was strongly suppressed in the LNT-229 rho^0-cells (Fig. 1a). In contrast, the expression of mitochondrial glutaminase 2 (GLS2), which is nuclear encoded was not affected by ethidium bromide treatment (Fig. 2a).

Furthermore, flow cytometry of TMRM stained cells and microscopic observation of CMXROS red staining revealed a reduction in mitochondrial membrane potential in LNT-229 rho^0-cells, while microscopic observation of mitotracker green staining was comparable in rho^0- and rho$^+$-cells (Fig. 2b–d). Mitotracker green stains free thiol groups of cystein residues belonging to mitochondrial proteins independent of the membrane potential and has been used to relate to mitochondrial mass (Agnello *et al.* 2008; Cottet-Rousselle *et al.* 2011). As expected, the disturbed mitochondrial function in the LNT-229 rho^0-cells was reflected by nearly complete suppression of oxygen consumption and lower reactive oxygen species levels (Fig. 2e–g).

In addition, these cells showed a more glycolytic phenotype with a higher lactate production (Fig. 3a). Furthermore, the expression of glucose transporter-1 and LDH-A was elevated in the LNT-229 rho^0-cells, indicating a more glycolytic phenotype (Fig 3b and c). In addition, we tested whether LNT-229 rho^0-cells were more susceptible towards glucose restriction and administration of 2DG, a competitive inhibitor of glycolysis. Cell growth inhibition under low glucose concentrations (1 mM) was aggravated in LNT-229 rho^0-cells, suggesting a higher glucose consumption of this cells compared to LNT-229 rho$^+$-cells. Interestingly, cell growth inhibition caused by 2DG was pronounced in rho^0- compared to rho$^+$-cells, while the combination of glucose restriction (1 mM) and 2DG was most effective (Fig. 3d).

LNT-229 rho^0-cells are resistant against hypoxia-induced cell death

We subsequently analysed whether adaptation to suppressed oxidative phosphorylation in LNT-229 rho^0-cells was associated to resistance against hypoxia. As shown in Fig. 4a, hypoxia-induced cell death was nearly completely abolished in the LNT-229 rho^0-cells. To further investigate whether resistance of LNT-229 rho^0-cells against hypoxia would translate in a relative growth advantage in a cell-competition assay, LNT-229 rho^0- and rho$^+$-cells were co-cultured under normoxia (5% O_2) and hypoxia (0.1% O_2). Although the proportion of LNT-229 rho^0- and rho$^+$-cells remained unaltered in normoxia, LNT-229 rho^0-cells strongly outnumbered LNT-229 rho$^+$-cells under hypoxia after 24 h (Fig. 4b). Together, these results suggest that LNT-229 rho^0-cells are resistant against hypoxia-induced cell death, providing these cells with a selective growth advantage under hypoxic conditions.

Rho^0-tumours are resistant against bevacizumab

Since suppression of oxidative phosphorylation caused resistance against hypoxia *in vitro*, we asked whether LNT-229 rho^0-tumours would be resistant to bevacizumab treatment *in vivo*. The expression of VEGF in the two cell lines was examined to analyse whether response to bevacizumab might be affected by different VEGF expression levels. No significant difference of VEGF expression on the mRNA level was observable between the two cell lines or subcutaneous xenografts (Fig. S1a). We also examined whether tumour growth rate was different between subcutaneous LNT-229 rho$^+$- and rho^0-tumour xenografts, and did not find a significant difference (Fig. S1b). To confirm *in vivo* persistence of the LNT-229 rho^0- phenotype, the expression of respiratory chain proteins was quantified via PCR in LNT-229 rho^0- and LNT-229 rho$^+$-subcutaneous xenografts. The

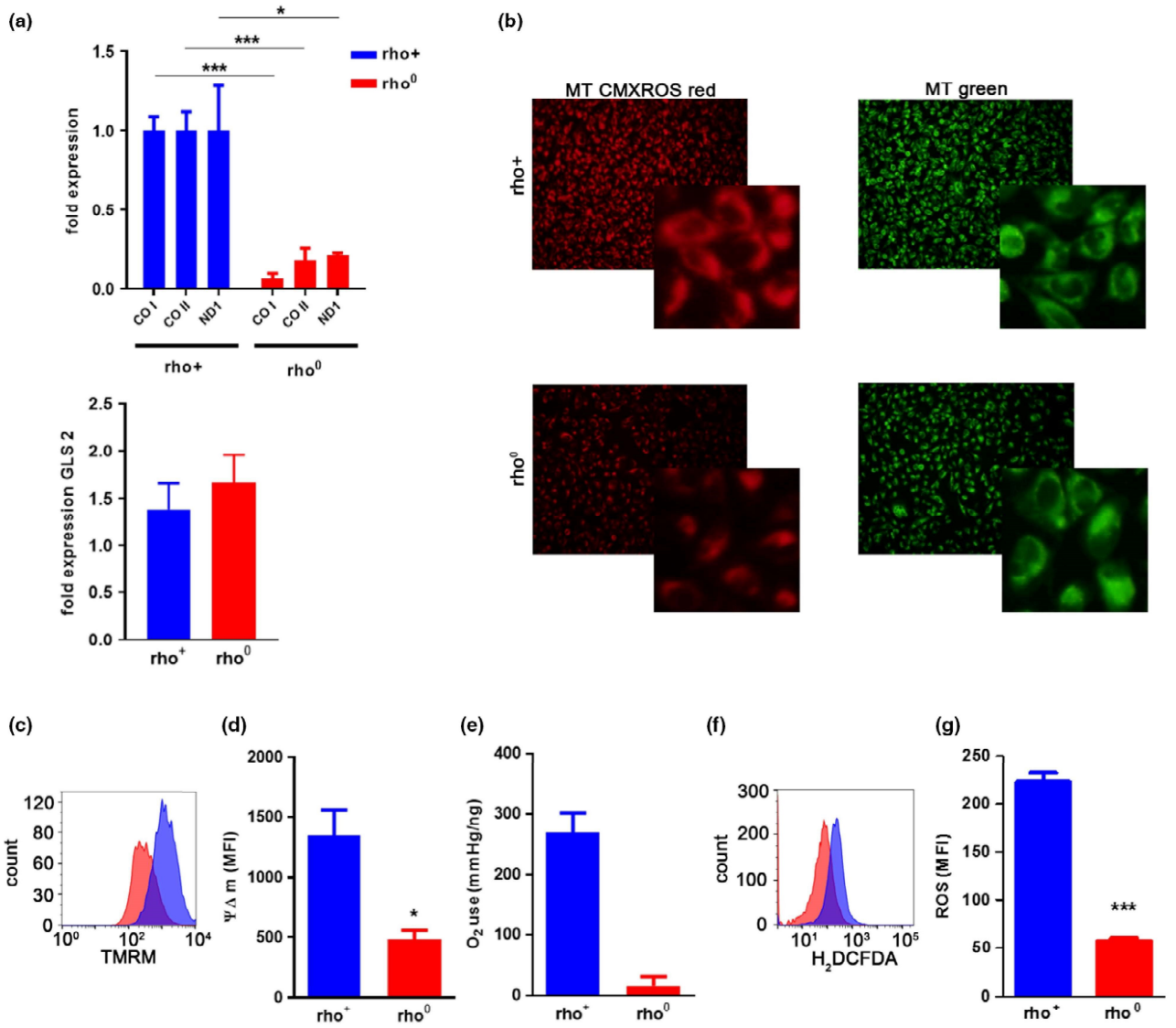

Fig. 2 LNT-229 rho^{0}cells have insufficient mitochondria and reduced oxidative phosphorylation. (a) LNT-229 rho$^+$- and LNT-229 rho^0-cells were cultivated as described in the methods section and expression of respiratory chain proteins CO I, (Cytochrome C oxidase I), CO II (Cytochrome C oxidase II), and ND1 (NADH dehydrogenase, subunit 1) as well as glutaminase 2 (GLS2) was analysed by q-PCR and expressed as relative expression ($2^{-(\Delta\Delta CT)}$). $N = 3$ replicates (b) Mitochondria in LNT-229 rho$^+$- and LNT-229 rho^0-cells were stained with mitotracker (MT) dependent (MT CMXRos) or independent (MT green) of the mitochondrial membrane potential, and representative photographs are shown. (c–d) The mitochondrial membrane potential was assessed by tetramethylrhodamine (TMRM) flow cytometry, $n = 6$ wells (c) representative histogram and (d) quantification of mean fluorescence intensity (MFI). (e) Oxygen consumption of LNT-229 rho$^+$- and rho^0-cells was determined. $N = 3$ replicates (f–g) reactive oxygen species (ROS) were quantified by H_2DCFDA flow cytometry analysis, $n = 3$ replicates (f) representative histogram and (g) quantification of MFI. Rho$^+$ cells are represented in blue and rho^0 cells in red. Shown are means ± SEM of triplicates, *$p < 0.05$, **$p < 0.001$, ***$p < 0.0001$, Student's *t*-test.

tumours formed from LNT-229 rho^0-cells had a persistently decreased expression of oxidative phosphorylation-related genes compared to LNT-229 rho$^+$-tumours (Fig. S1c).

Like the *in vitro* results, LDH-A expression was increased in rho^0- compared to rho$^+$-tumours in orthotopic xenografts (Fig. 5a), indicating that LNT-229 rho^0-tumours retained the metabolic phenotype *in vivo*. Finally, sensitivity of LNT-229 rho^0- and rho$^+$-tumours against bevacizumab was analysed. While bevacizumab prolonged survival of mice bearing intracranial LNT-229 rho$^+$-tumours (74 days vs. 105 days, $p = 0.024$ log-rank test), it had no effect on survival in mice carrying LNT-229 rho^0-tumours (75 days vs. 70 days, $p = 0.52$ log-rank test) (Fig. 5b). The histological analysis of untreated rho$^+$- or rho^0-tumours did not reveal considerable differences (Fig. 5c). Bevacizumab induced hypoxia in rho$^+$- as well as rho^0- tumours, as displayed by an increase in

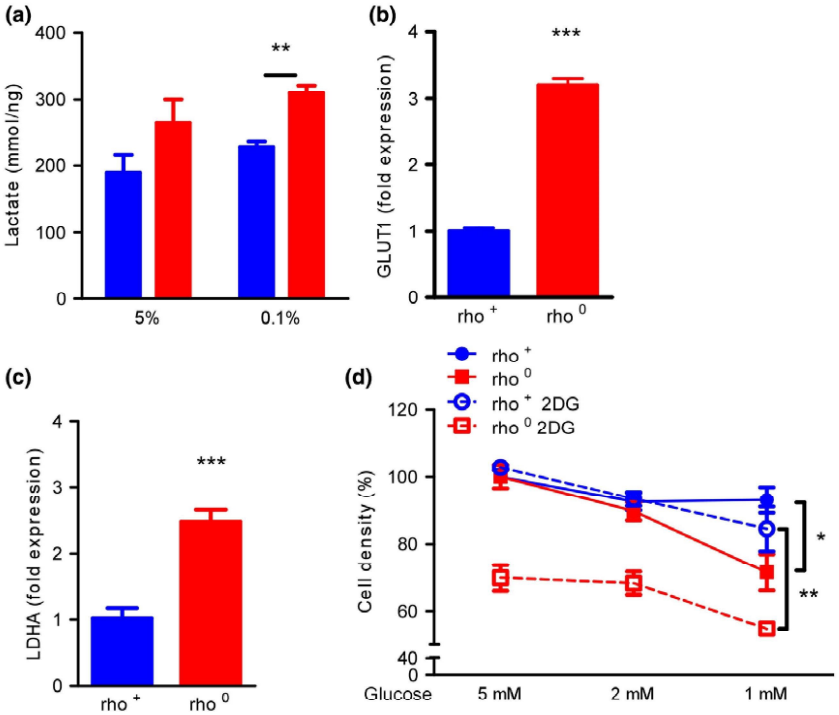

Fig. 3 Increased glycolysis in LNT-229 rho^0-cells. (a) Lactate production was quantified in LNT-229 rho$^+$- and LNT-229 rho^0-cells after 72 h. $N = 3$ wells (b) Expression of glucose transporter-1 (GLUT1) and of (c) Lactate dehydrogenase A (LDH-A) was analysed by q-PCR and expressed as relative expression. $N = 3$ replicates (d) Relative cell density after incubation for 12 h in the absence or presence of 2DG (5 mM) and different glucose concentrations (1–5 mM) was assessed by crystal violet staining and expressed as percent of staining under standard conditions (5 mM glucose without 2DG), $n = 6$ wells. Rho$^+$ is represented in blue (dark) and rho^0 in red (bright). Shown are means ± SEM of triplicates, $*p < 0.05$, $**p < 0.001$, $***p < 0.0001$, Student's *t*-test.

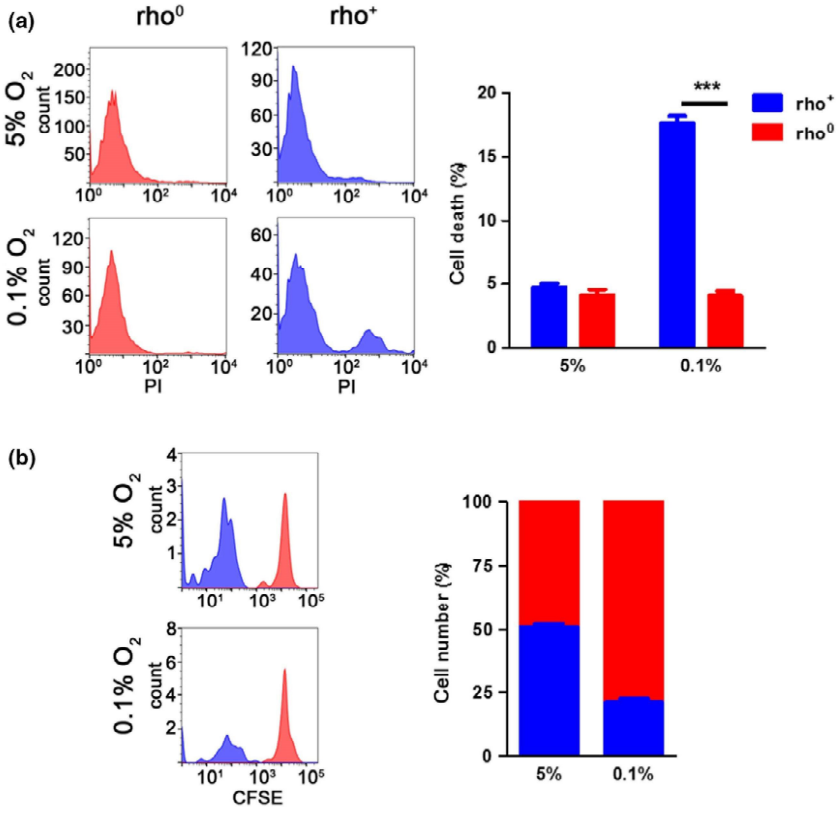

Fig. 4 LNT-229 rho^0-cells are resistant to hypoxia. (a) Cells were exposed to 5% O_2 or 0.1% O_2 for 24 h, and cell death was analysed by PI-flow cytometry. (Left) representative flow cytometry histograms, (right) quantification of PI positive cells. $N = 3$ wells (b) CFSE-stained LNT-229 rho^0-cells and unstained LNT-229 rho$^+$-cells were mixed in a 1 : 1 ratio and incubated for 24 h at 5% or 0.1% O2. The relative amount of LNT-229 rho^0- and rho$^+$-cells was quantified by flow cytometry. (Left) representative flow cytometry histograms, (right) quantification of PI positive cells, $n = 3$ wells. Rho$^+$ is represented in blue (dark) and rho^0 in red (bright). Shown are means ± SEM of triplicates, $*p < 0.05$, $**p < 0.001$, $***p < 0.0001$, student's *t*-Test.

HIF-1α accumulation and translocation to the cell nucleus after bevacizumab treatment (Fig. 5d). No differences in the extent of necrotic foci were seen, and glial fibrillary acidic protein expression in residual murine brain tissues was similar showing increased immunoreactivity in close vicinity to the tumour border (data not shown).

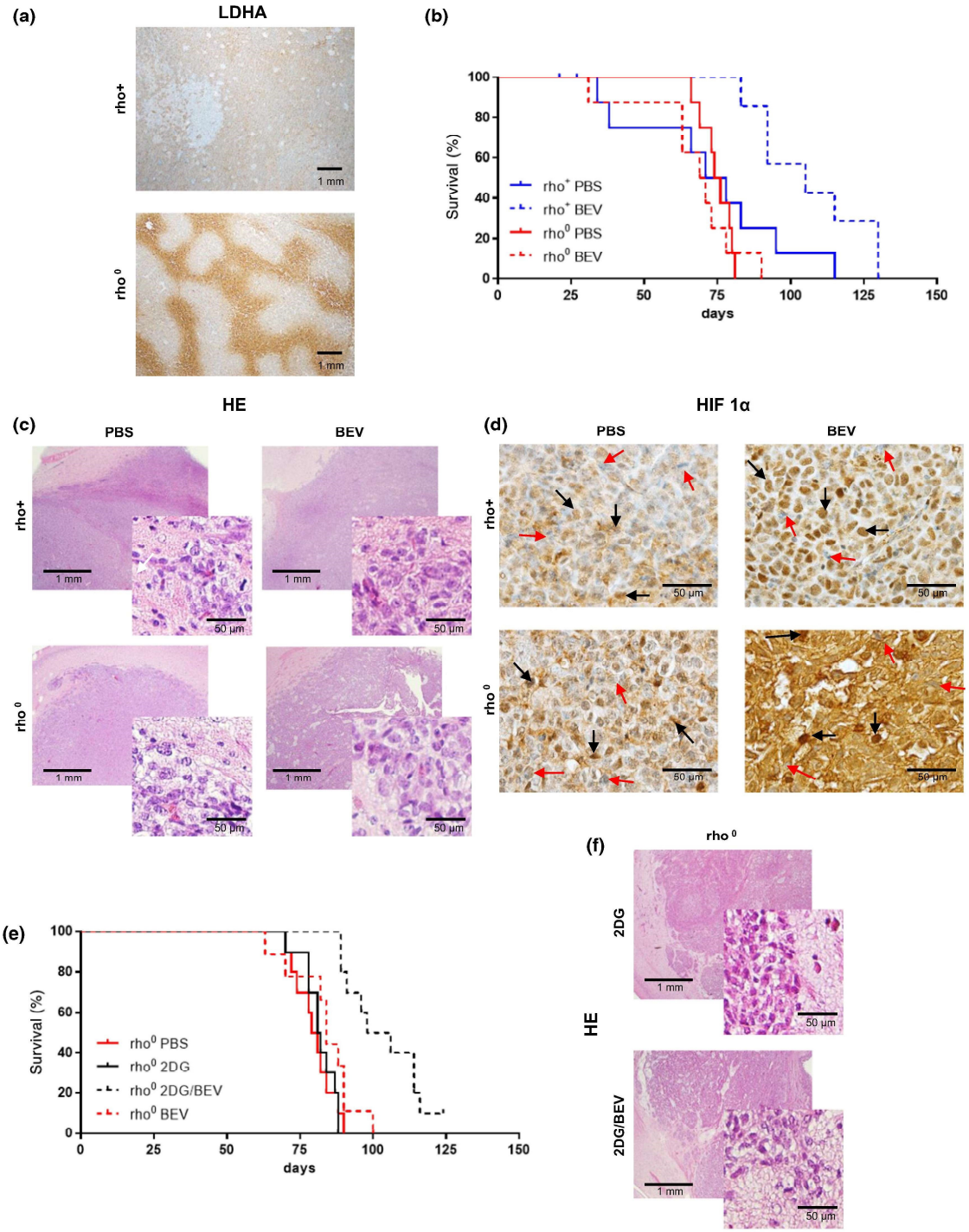

Fig. 5 Rho^0-tumours are resistant against bevacizumab and sensitive to 2DG. (a) LNT-229 rho$^+$- and rho^0-cells were intracranial implanted in nude mice, $n = 9$. Lactate dehydrogenase A (LDH-A) expression was analysed by immunohistochemistry. (b) 7 d after implantation, treatment with phosphate buffered saline (PBS) or bevacizumab was started and survival was analysed by Kaplan–Meier-statistic. (c) Representative sections of rho$^+$- and rho^0-tumours treated with PBS were stained with hematoxylin eosin (HE). (d) Sections were labelled with HIF 1α and nuclear translocation of the transcription factor was observed (black arrows HIF 1α positive nuclei, red arrows HIF 1α negative nuclei). (e) Mice barring intracranial rho^0-tumours were treated with 2DG or PBS at day 7–9. $N = 9$. From day 10, PBS, bevacizumab and/or 2DG was administered twice a week and survival was analysed by Kaplan–Meier-analysis. (f) Representative sections of rho^0 cells treated with 2DG only or the combination of 2DG and bevacizumab were stained with HE.

2DG restores sensitivity of rho^0-tumours against bevacizumab

As LNT-229 rho^0-cells were glucose-addicted and hypersensitive to 2DG *in vitro*, we asked whether 2DG would be able to rescue their resistance towards bevacizumab *in vivo*. Indeed, whereas neither treatment with 2DG (81 days vs. 80 days, $p = 0.85$) nor bevacizumab alone (81 days vs. 84 days, $p = 0.13$) improved the median survival compared to PBS, the combination of bevacizumab and 2DG showed a synergistic effect and prolonged the median survival by 22% compared to the PBS treated group (98 days vs. 80 days, $p = 0.0001$) (Fig. 5e). No relevant differences in tumour morphology were observed between 2DG-treated rho^0-cells as compared to their counterparts with additional bevacizumab treatment (Fig. 5f).

Discussion

Understanding mechanisms of resistance against antiangiogenic therapies is of great interest because in gliomas, antiangiogenic drugs such as bevacizumab and cediranib do not result in sustained benefit and bevacizumab-resistant tumours are highly refractory to conventional therapies. Considering that these agents induce vessel rarefication (Baumgarten *et al.* 2011) and hypoxia (Xu *et al.* 2015), it appears plausible that therapy resistance involves adaptation of tumour cells to hypoxic conditions. A possible major mechanism of resistance against hypoxia is that tumour cells undergo a metabolic switch from oxidative phosphorylation towards glycolysis. Indeed, Fack *et al.* (2015) recently showed that treatment with bevacizumab led to a more glycolytic phenotype in glioma xenograft tumours as reflected by an increase in glucose flux and lactate production. Similarly, in ovarian cancer xenografts, bevacizumab led to the emergence of cancer cells showing reduced oxidative phosphorylation and increased glucose utilization and lactate production (Curtarello *et al.* 2015). The importance of increased glycolysis as a mediator of bevacizumab-resistance is suggested by the finding that, in colorectal cancer, higher expression of glycolytic genes was associated with a worse prognosis in patients treated with bevacizumab and chemotherapy (Graziano *et al.* 2016). Together, these results indicate that tumour cells undergo a metabolic switch towards glycolysis during bevacizumab therapy. As it is likely that glycolysis is enhanced under hypoxic conditions, it remained unclear if increased glycolysis is a prerequisite to bevacizumab resistance or an epiphenomenon as a result of the therapy-induced hypoxia. We now demonstrate that suppression of oxidative phosphorylation in rho^0-cells accompanied by enforced glycolysis is sufficient to induce resistance against bevacizumab (Fig. 5). Together, these observations demonstrate that the recent findings of a metabolic switch towards glycolysis in bevacizumab-treated tumours are indeed causative to resistance against antiangiogenic therapies. How this metabolic switch exactly occurs remains unclear but might be a consequence of a selective pressure on oxic tumour cells.

As rho^0-cells are highly resistant against hypoxic conditions (Fig. 4), these results strengthen the assumption that bevacizumab impairs tumour growth at least partly by induction of hypoxia. Conversely, treatment with anti-angiogenic agents would lead to a selection pressure favouring the survival of glycolytic and hypoxia-resistant tumour cells.

The increased dependency of these tumours on glycolysis suggests that targeting glucose metabolism is a promising strategy to circumvent bevacizumab-resistance. Indeed, while 2DG alone did not affect tumour growth, the combination of bevacizumab with 2DG was effective in the treatment of bevacizumab resistant LNT-229 rho^0 -tumours (Fig. 5). *In vitro*, the effect of 2DG on cell proliferation was dependent on the ratio between glucose and 2DG, and the combination of glucose restriction together with 2DG treatment was most effective to inhibit proliferation of LNT-229-rho^0-cells (Fig. 3d). It could therefore be speculated that in 2DG-alone treated tumours, blood vessels and glucose supply were not decreased, and that persistent high glucose levels in the tumours result in antagonism of the growth-inhibitory effects of 2DG that are sufficient even for the higher glucose needs of rho^0-cells. Treatment with bevacizumab might cause a shortage of glucose in the tumours by reducing blood flow as well as vessel permeability and increasing glucose consumption (Fack *et al.* 2015). Because 2DG accumulates in the tumour cells (Pelicano *et al.* 2006), 2DG levels in tumours might be less affected by bevacizumab compared to glucose levels, raising the 2DG to glucose ratio above the threshold necessary for growth inhibition.

Together, our results demonstrate that increased glycolysis and resistance towards hypoxia are sufficient to induce a bevacizumab-resistant phenotype in an experimental glioma model. The assumption that increasing glycolysis is a mechanism of resistance against antiangiogenic therapies is supported by the finding that glucose restriction by a ketogenic diet increased the activity of bevacizumab in a mouse xenograft model (Rieger *et al.* 2014). Inhibiting glucose metabolism by either glycolysis inhibitors or glucose restriction might therefore be a promising strategy to improve the efficacy of antiangiogenic therapies.

Acknowledgments and conflict of interest disclosure

The work was supported by grant RI2175/1-1 from the "Deutsche Forschungsgemeinschaft" (DFG) to JPS and JR. The Dr Senckenberg Institute of Neurooncology is supported by the Hertie foundation and the Dr Senckenberg foundation. JPS is "Hertie Professor for Neurooncology". The authors declare no conflict of interest.

All experiments were conducted in compliance with the ARRIVE guidelines.

Supporting information

Additional Supporting Information may be found online in the supporting information tab for this article:

Figure S1. Rho^0 cells have a stable phenotype throughout the in-vitro experiment but no alterations in VEGF expression or growth behavior.

References

Agnello M., Morici G. and Rinaldi A. M. (2008) A method for measuring mitochondrial mass and activity. *Cytotechnology* **56**, 145–149.

Bahr O., Hattingen E., Rieger J. and Steinbach J. P. (2011) Bevacizumab-induced tumor calcifications as a surrogate marker of outcome in patients with glioblastoma. *Neuro. Oncol.* **13**, 1020–1029.

Baumgarten L. V., Brucker D., Tirniceru A., Kienast Y., Grau S., Burgold S., Herms J. and Winkler F. (2011) Bevacizumab has differential and dose-dependent effects on glioma blood vessels and tumor cells. *Clinical Cancer Research*, **17**, 6192–6205.

Berger B., Capper D., Lemke D., Pfenning P. N., Platten M., Weller M., von Deimling A., Wick W. and Weiler M. (2010) Defective p53 antiangiogenic signaling in glioblastoma. *Neuro. Oncol.* **12**, 894–907.

Bergers G. and Hanahan D. (2008) Modes of resistance to anti-angiogenic therapy. *Nat. Rev. Cancer* **8**, 592 603.

Chinot O. L., Wick W., Mason W. *et al.* (2014) Bevacizumab plus radiotherapy-temozolomide for newly diagnosed glioblastoma. *N. Engl. J. Med.* **370**, 709–722.

Cottet-Rousselle C., Ronot X., Leverve X. and Mayol J. F. (2011) Cytometric assessment of mitochondria using fluorescent probes. *Cytometry A* **79**, 405–425.

Curtarello M., Zulato E., Nardo G. *et al.* (2015) VEGF-targeted therapy stably modulates the glycolytic phenotype of tumor cells. *Can. Res.* **75**, 120–133.

DeLay M., Jahangiri A., Carbonell W. S., Hu Y.-L., Tsao S., Tom M. W., Paquette J., Tokuyasu T. A. and Aghi M. K. (2012) Microarray analysis verifies two distinct phenotypes of glioblastomas resistant to antiangiogenic therapy. *Clin. Cancer Res.* **18**, 2930–2942.

Fack F., Espedal H., Keunen O. *et al.* (2015) Bevacizumab treatment induces metabolic adaptation toward anaerobic metabolism in glioblastomas. *Acta Neuropathol.* **129**, 115–131.

Favaro E., Bensaad K., Chong M. G. *et al.* (2012) Glucose utilization via glycogen phosphorylase sustains proliferation and prevents premature senescence in cancer cells. *Cell Metab.* **16**, 751–764.

Friedman H. S., Prados M. D., Wen P. Y. *et al.* (2009) Bevacizumab alone and in combination with irinotecan in recurrent glioblastoma. *J. Clin. Oncol.* **27**, 4733–4740.

Gilbert M. R., Dignam J. J., Armstrong T. S. *et al.* (2014) A randomized trial of bevacizumab for newly diagnosed glioblastoma. *N. Engl. J. Med.* **370**, 699–708.

Graziano F., Ruzzo A., Giacomini E. *et al.* (2016) Glycolysis gene expression analysis and selective metabolic advantage in the clinical progression of colorectal cancer. *Pharmacogenomics J.* **17**, 258–264.

de Groot J. F., Fuller G., Kumar A. J., Piao Y., Eterovic K., Ji Y. and Conrad C. A. (2010) Tumor invasion after treatment of glioblastoma with bevacizumab: radiographic and pathologic correlation in humans and mice. *Neuro. Oncol.* **12**, 233–242.

Jahangiri A., Lay M. D., Miller L. M. *et al.* (2013) Gene expression profile identifies tyrosine kinase c-Met as a targetable mediator of antiangiogenic therapy resistance. *Clin. Cancer Res.*, **19**, 1773–1783.

Jain R. K. (2014) Antiangiogenesis strategies revisited: from starving tumors to alleviating hypoxia. *Cancer Cell* **26**, 605–622.

Keunen O., Johansson M., Oudin A. *et al.* (2011) Anti-VEGF treatment reduces blood supply and increases tumor cell invasion in glioblastoma. *Proc. Natl Acad. Sci. USA* **108**, 3749–3754.

Kreisl T. N., Kim L., Moore K. *et al.* (2009) Phase II trial of single-agent bevacizumab followed by bevacizumab plus irinotecan at tumor progression in recurrent glioblastoma. *J. Clin. Oncol.* **27**, 740–745.

Kueng W., Silber E. and Eppenberger U. (1989) Quantification of cells cultured on 96-well plates. *Anal. Biochem.* **182**, 16–19.

Lee M., Muller F., Aquilanti E., Hu B. and DePinho R. (2012) Stereotactic orthotopic xenograft injections into the mouse brain. *Nature Protocol Exchange* doi:10.1038/protex.2012.041

McKeown S. R. (2014) Defining normoxia, physoxia and hypoxia in tumours-implications for treatment response. *Br. J. Radiol.* **87**, 20130676.

Miller S. W., Trimmer P. A., Parker W. D., Jr and Davis R. E. (1996) Creation and characterization of mitochondrial DNA-depleted cell lines with "neuronal-like" properties. *J. Neurochem.* **67**, 1897–1907.

Nanegrungsunk D., Apaijai N., Yarana C., Sripetchwandee J., Limpastan K., Watcharasaksilp W., Vaniyapong T., Chattipakorn N. and Chattipakorn S. C. (2016) Bevacizumab is superior to Temozolomide in causing mitochondrial dysfunction in human brain tumors. *Neurol. Res.* **38**, 285–293.

Pelicano H., Martin D. S., Xu R.-H. and Huang P. (2006) Glycolysis inhibition for anticancer treatment. *Oncogene* **25**, 4633–4646.

Rahman R., Hempfling K., Norden A. D. *et al.* (2014) Retrospective study of carmustine or lomustine with bevacizumab in recurrent glioblastoma patients who have failed prior bevacizumab. *Neuro. Oncol.* **16**, 1523–1529.

Rieger J., Bähr O., Müller K., Franz K., Steinbach J. and Hattingen E. (2010) Bevacizumab-induced diffusion-restricted lesions in malignant glioma patients. *J. Neurooncol.* **99**, 49–56.

Rieger J., Bähr O., Maurer G. D. *et al.* (2014) ERGO: a pilot study of ketogenic diet in recurrent glioblastoma. *Int. J. Oncol.* **44**, 1843–1852.

Thiepold A. L., Lorenz N., Foltyn M. *et al.* (2017) Mammalian target of rapamycin complex 1 activation sensitizes human glioma cells to hypoxia-induced cell death. *Brain* **140**, 10.

Vandesompele J., De Preter K., Pattyn F., Poppe B., Van Roy N., De Paepe A. and Speleman F. (2002) Accurate normalization of real-time quantitative RT-PCR data by geometric averaging of multiple internal control genes. *Genome Biol.* **3**, 35.

Wanka C., Steinbach J. P. and Rieger J. (2012) Tp53-induced glycolysis and apoptosis regulator (TIGAR) protects glioma cells from starvation-induced cell death by up-regulating respiration and improving cellular redox homeostasis. *J. Biol. Chem.* **287**, 33436–33446.

Wischhusen J., Naumann U., Ohgaki H., Rastinejad F. and Weller M. (2003) CP-31398, a novel p53-stabilizing agent, induces p53-dependent and p53-independent glioma cell death. *Oncogene* **22**, 8233–8245.

Xu J., Wang J., Xu B., Ge H., Zhou X. and Fang J.-Y. (2013) Colorectal cancer cells refractory to anti-VEGF treatment are vulnerable to glycolytic blockade due to persistent impairment of mitochondria. *Mol. Cancer Ther.* **12**, 717–724.

Xu H., Rahimpour S., Nesvick C. L. *et al.* (2015) Activation of hypoxia signaling induces phenotypic transformation of glioma cells: implications for bevacizumab antiangiogenic therapy. *Oncotarget* **14**, 11882–11893.

Darstellung des eigenen Anteils an der Publikation

Die Projektplanung erfolgte gemeinsam mit Johannes Rieger, Joachim Steinbach und Christina Wanka.

Die *in-vitro* Experimente wurden selbstständig geplant und durchgeführt, ausgenommen der GLS2 Expression (Abbildung 1A unten), die durch Ines Bruns durchgeführt wurde; sowie der Bestimmung des mitochondrialen Membranpotentials, der Bestimmung der ROS Produktion (Abbildung 1 C-G) und der Laktat-Produktion (Abbildung 2 A), diese erfolgten durch Christina Wanka. Die Histologie erfolgte in Zusammenarbeit mit Janusz von Renesse, Patrick Harter und Michel Mittelbronn (Abbildung 4 A, C, D, F).

Alle *in-vivo* Experimente wurden selbstständig geplant und durchgeführt. Das subkutane Tiermodell wurde in Zusammenarbeit mit Hans Urban durchgeführt. Die intrakranielle Tumorimplantation erfolgte unter Mithilfe von Michael Burger.

Das Manuskript wurde selbstständig verfasst und gemeinsam mit Johannes Rieger und Joachim Steinbach fertiggestellt.

Abschießende Zusammenfassung

Neue Studien konnten zeigen, dass mit Bevacizumab behandelte Glioblastome vermehrt Enzyme der glykolytischen Energiegewinnung exprimieren [6]. Außerdem konnte gezeigt werden, dass Glioblastome auch nach Erlangen einer Bevacizumabresistenz noch eine verminderte Gefäßdichte aufweisen sowie vermehrt Hypoxiemarker exprimieren [28].

Da eine vermehrte Glykolyse einen metabolischen Vorteil unter hypoxischen Bedingungen darstellt war die Fragestellung der hier vorliegenden Arbeit, ob in Glioblastomzellen allein die Umstellung des Zellmetabolismus auf rein glykolytische Energiegewinnung eine Hypoxieresistenz und somit eine Resistenz gegenüber Bevacizumab hervorrufen kann. Obwohl ein Zusammenhang zwischen Resistenzentwicklung und vermehrter Glykolyse nahezuliegen scheint, wurde der Kausalzusammenhang bisher nicht untersucht. Die Ergebnisse dieser Arbeit zeigen, dass die alleinige Depletion mitochondrialer Atmungskettenbestandteile einen

glykolytischen Phänotyp in der Glioblastom Zelllinie LNT-229 hervorruft und eine Hypoxieresistenz verursacht. Diese glykolytischen Glioblastomzellen wiesen außerdem eine Bevacizumabresistenz in Tumor-Xenografts bei Mäusen auf. Die Ergebnisse lassen somit vermuten, dass alleine die metabolische Umstellung hin zu einer glykolytischen Energiegewinnung und somit Unabhängigkeit von Sauerstoff eine Bevacizumabresistenz bedingen kann. Die bereits in anderen Studien beschriebenen metabolischen Veränderungen in Bevacizumab-resistenten Glioblastomen scheinen somit in direktem kausalen Zusammenhang mit der Resistenzentwicklung zu stehen. Der Zellmetabolismus stellt deshalb einen wichtigen Angriffspunkt zur Vorbeugung und Behandlung von Bevacizumabresistenzen Tumoren dar. Die Ergebnisse dieser Studie zeigen weiterhin, dass eine Kombination von Bevacizumab mit dem Glykolyse-Inhibitor 2DG die Resistenz zumindest teilweise aufheben konnte. Dieses Ergebnis unterstützt weitere therapeutische Ansätze, Bevacizumab-Behandlung durch die Beeinflussung des Zellmetabolismus zu verbessern.

Literaturverzeichnis

1. Kong D-H, Kim MR, Jang JH, Na H-J, Lee S. A Review of Anti-Angiogenic Targets for Monoclonal Antibody Cancer Therapy. *Int J Mol Sci*. 2017;18(8). doi:10.3390/ijms18081786.

2. Gilbert MR, Dignam JJ, Armstrong TS, et al. A randomized trial of bevacizumab for newly diagnosed glioblastoma. *N Engl J Med*. 2014;370(8):699-708. doi:10.1056/NEJMoa1308573.

3. Keunen O, Johansson M, Oudin A, et al. Anti-VEGF treatment reduces blood supply and increases tumor cell invasion in glioblastoma. *Proc Natl Acad Sci U S A*. 2011;108(9):3749-3754. doi:10.1073/pnas.1014480108.

4. Hattingen E, Jurcoane A, Bähr O, et al. Bevacizumab impairs oxidative energy metabolism and shows antitumoral effects in recurrent glioblastomas: A 31P/1H MRSI and quantitative magnetic resonance imaging study. *Neuro-oncology*. 2011;13(12):1349-1363. doi:10.1093/neuonc/nor132.

5. Baumgarten L von, Brucker D, Tirniceru A, et al. Bevacizumab has differential and dose-dependent effects on glioma blood vessels and tumor cells. *Clin Cancer Res*. 2011;17(19):6192-6205. doi:10.1158/1078-0432.CCR-10-1868.

6. Fack F, Espedal H, Keunen O, et al. Bevacizumab treatment induces metabolic adaptation toward anaerobic metabolism in glioblastomas. *Acta Neuropathol*. 2015;129(1):115-131. doi:10.1007/s00401-014-1352-5.

7. Curtarello M, Zulato E, Nardo G, et al. VEGF-targeted therapy stably modulates the glycolytic phenotype of tumor cells. *Cancer Res*. 2015;75(1):120-133. doi:10.1158/0008-5472.CAN-13-2037.

8. Xu J, Wang J, Xu B, Ge H, Zhou X, Fang J-Y. Colorectal cancer cells refractory to anti-VEGF treatment are vulnerable to glycolytic blockade due to persistent impairment of mitochondria. *Mol Cancer Ther*. 2013;12(5):717-724. doi:10.1158/1535-7163.MCT-12-1016-T.

9. Nanegrungsunk D, Apaijai N, Yarana C, et al. Bevacizumab is superior to Temozolomide in causing mitochondrial dysfunction in human brain tumors. *Neurol Res*. 2016;38(4):285-293. doi:10.1080/01616412.2015.1114233.

10. Schwartzbaum JA, Fisher JL, Aldape KD, Wrensch M. Epidemiology and molecular pathology of glioma. *Nat Clin Pract Neurol*. 2006;2(9):494-503; quiz 1 p following 516. doi:10.1038/ncpneuro0289.

11. Ishii N, Maier D, Merlo A, et al. Frequent co-alterations of TP53, p16/CDKN2A, p14ARF, PTEN tumor suppressor genes in human glioma cell lines. *Brain Pathol*. 1999;9(3):469-479.

12. Stupp R, Mason WP, van den Bent MJ, et al. Radiotherapy plus concomitant and adjuvant temozolomide for glioblastoma. *N Engl J Med*. 2005;352(10):987-996. doi:10.1056/NEJMoa043330.

13. Weller M, Cloughesy T, Perry JR, Wick W. Standards of care for treatment of recurrent glioblastoma--are we there yet? *Neuro-oncology*. 2013;15(1):4-27. doi:10.1093/neuonc/nos273.

14. Field KM, Simes J, Nowak AK, et al. Randomized phase 2 study of carboplatin and bevacizumab in recurrent glioblastoma. *Neuro-oncology*. 2015;17(11):1504-1513. doi:10.1093/neuonc/nov104.

15. Hennipman A, van Oirschot BA, Smits J, Rijksen G, Staal GE. Glycolytic enzyme activities in breast cancer metastases. *Tumour Biol*. 1988;9(5):241-248.

16. Goldman RD, Kaplan NO, Hall TC. Lactic dehydrogenase in human neoplastic tissues. *Cancer Res*. 1964;24:389-399.

17. Favaro E, Bensaad K, Chong MG, et al. Glucose utilization via glycogen phosphorylase sustains proliferation and prevents premature senescence in cancer cells. *Cell Metab*. 2012;16(6):751-764. doi:10.1016/j.cmet.2012.10.017.

18. Miranda-Gonçalves V, Cardoso-Carneiro D, Valbom I, et al. Metabolic alterations underlying Bevacizumab therapy in glioblastoma cells. *Oncotarget*. 2017;8(61):103657-103670. doi:10.18632/oncotarget.21761.

19. WARBURG O. On respiratory impairment in cancer cells. *Science*. 1956;124(3215):269-270.

20. Macheda ML, Rogers S, Best JD. Molecular and cellular regulation of glucose transporter (GLUT) proteins in cancer. *J Cell Physiol*. 2005;202(3):654-662. doi:10.1002/jcp.20166.

21. Rieger J, Bähr O, Maurer GD, et al. ERGO: A pilot study of ketogenic diet in recurrent glioblastoma. *Int J Oncol*. 2014;44(6):1843-1852. doi:10.3892/ijo.2014.2382.

22. Kumar K, Wigfield S, Gee HE, et al. Dichloroacetate reverses the hypoxic adaptation to bevacizumab and enhances its antitumor effects in mouse xenografts. *J Mol Med*. 2013;91(6):749-758. doi:10.1007/s00109-013-0996-2.

23. Zhang D, Li J, Wang F, Hu J, Wang S, Sun Y. 2-Deoxy-D-glucose targeting of glucose metabolism in cancer cells as a potential therapy. *Cancer Lett*. 2014;355(2):176-183. doi:10.1016/j.canlet.2014.09.003.

24. Dwarakanath BS, Singh D, Banerji AK, et al. Clinical studies for improving radiotherapy with 2-deoxy-D-glucose: Present status and future prospects. *J Cancer Res Ther*. 2009;5 Suppl 1:S21-6. doi:10.4103/0973-1482.55136.

25. Chinot OL, Wick W, Mason W, et al. Bevacizumab plus radiotherapy-temozolomide for newly diagnosed glioblastoma. *N Engl J Med*. 2014;370(8):709-722. doi:10.1056/NEJMoa1308345.

26. Friedman HS, Prados MD, Wen PY, et al. Bevacizumab alone and in combination with irinotecan in recurrent glioblastoma. *J Clin Oncol*. 2009;27(28):4733-4740. doi:10.1200/JCO.2008.19.8721.

27. Bergers G, Hanahan D. Modes of resistance to anti-angiogenic therapy. *Nat Rev Cancer*. 2008;8(8):592-603. doi:10.1038/nrc2442.

28. Yamamoto Y, Tamura R, Tanaka T, et al. "Paradoxical" findings of tumor vascularity and oxygenation in recurrent glioblastomas refractory to bevacizumab. *Oncotarget.* 2017; 8(61):103890-103899.

doi: 10.18632/oncotarget.21978.

29. Taphoorn MJB, Henriksson R, Bottomley A, et al. Health-Related Quality of Life in a Randomized Phase III Study of Bevacizumab, Temozolomide, and Radiotherapy in Newly Diagnosed Glioblastoma. Journal of Clinical Oncology. 2015;33(19):2166-2175. doi:10.1200/JCO.2014.60.3217.

30. Wick W, Brandes AA, Gorlia T, et al. EORTC 26101 phase III trial exploring the combination of bevacizumab and lomustine in patients with first progression of a glioblastoma. Journal of Clinical Oncology. 2016;34(15_suppl):2001. doi:10.1200/JCO.2016.34.15_suppl.2001.

31. Gramatzki D, Roth P, Rushing EJ, et al. Bevacizumab may improve quality of life, but not overall survival in glioblastoma: An epidemiological study. Ann Oncol. 2018;29(6):1431-1436. doi:10.1093/annonc/mdy106.

Schriftliche Erklärung

Ich erkläre ehrenwörtlich, dass ich die dem Fachbereich Medizin der Johann Wolfgang Goethe-Universität Frankfurt am Main zur Promotionsprüfung eingereichte Dissertation mit dem Titel

Hemmung der oxidativen Phosphorylierung führt zu Bevacizumabresistenz in Glioblastomzellen

in der Klinik für Neurologie, Funktionsbereich Neuroonkologie, unter Betreuung und Anleitung von Prof Dr. med. Joachim P. Steinbach, mit Unterstützung durch Herrn PD Dr. med. Johannes Rieger, ohne sonstige Hilfe selbst durchgeführt und bei der Abfassung der Arbeit keine anderen als die in der Dissertation angeführten Hilfsmittel benutzt habe. Darüber hinaus versichere ich, nicht die Hilfe einer kommerziellen Promotionsvermittlung in Anspruch genommen zu haben.
Die vorliegende Arbeit wurde bisher nicht als Dissertation eingereicht.
Vorliegende Ergebnisse der Arbeit wurden in folgendem Publikationsorgan veröffentlicht:

Eriksson JA, Wanka C, Burger MC, Urban H, Hartel I, von Renesse J, Harter PN, Mittelbronn M, Steinbach JP, Rieger J. Suppression of oxidative phosphorylation confers resistance against bevacizumab in experimental glioma. J Neurochem. 144(4):421-430; 2018.

(Ort, Datum) (Unterschrift)